

Electrocoalescence of drops synchronized by size-dependent flow in microfluidic channels

Keunho Ahn and Jeremy Agresti

DEAS, Harvard University, Cambridge, Massachusetts 02138 and Interdisciplinary Network of Emerging Science and Technology (INEST) Group, Research Center, Philip Morris USA, Richmond, Virginia 23224

Henry Chong

DEAS, Harvard University, Cambridge, Massachusetts 02138

Manuel Marquez

Harrington Department of Bioengineering, Arizona State University, Tempe, Arizona 85287-9709 and Interdisciplinary Network of Emerging Science and Technology (INEST) Group, Research Center, Philip Morris USA, Richmond, Virginia 23224

D. A. Weitz^{a)}

DEAS, Harvard University, Cambridge, Massachusetts 02138 and Department of Physics, Harvard University, Cambridge, Massachusetts 02138

(Received 4 April 2006; accepted 15 May 2006; published online 29 June 2006)

The use of microfluidic devices to control drops of water in a carrier oil is a promising means of performing biological and chemical assays. An essential requirement for this is the controlled coalescence of pairs of drops to mix reagents together. We show that this can be accomplished through electrocoalescence of drops synchronized by size-dependent flow in microfluidic channels. Smaller drops move faster due to the Poiseuille flow, allowing pairs of surfactant-stabilized drops to be brought into contact where they are coalesced with an electric field. We apply this method to an enzyme assay to measure enzyme kinetic constants. © 2006 American Institute of Physics.
[DOI: 10.1063/1.2218058]

Microfluidic devices are a promising platform for novel, high-throughput chemical and biological assays. One method for isolating and controlling small quantities of reagents is through the use of small surfactant-stabilized drops of water in a carrier oil, where each drop acts as a small picoliter-volume microreactor. An essential function required for truly general assays is the precise combination of reagents; this is best achieved through the controlled coalescence of pairs of droplets. Such controlled, high speed coalescence of drops containing different materials would be important for many chemical and biochemical applications such as particle synthesis, enzyme assays, enzyme inhibitor assays, and protein translation assays in microfluidic systems. However, controlled coalescence of surfactant-stabilized droplets is difficult: for drops to coalesce, it is necessary for them to touch or be close enough to force them to touch. A one-to-one correspondence between the microreactor drop and the additive drop requires the spacing and period between drops to be precisely synchronized in space and time. Coalescence of drops has been demonstrated for drops that are not surfactant stabilized.^{1,2} Another scheme has used oppositely charged drops formed simultaneously and merged and coalesced by their charges.³ Alternate drop formation was used for electrocoalescence of two adjacent drops that were brought together by introducing them into a wider channel.⁴ In both these schemes, the range over which drops can be synchronized is limited to the region of the device where the drops are formed and are thus still periodic and well spaced. The difficulty of controllably combining pairs of drops at arbitrary

points has limited the widespread use of droplet microreactors in microfluidic devices.

In this letter, we describe controlled, high-throughput coalescence of droplets within a microfluidic device. We exploit the fact that smaller drops flow at higher velocities than larger drops due to the parabolic flow velocity distribution in microfluidic channels. Two streams of different-sized drops made independently with different time scales, sizes, and compositions are merged in a single microfluidic channel. The small drops catch up to and come in contact with the larger drops, but do not coalesce when they are stabilized with surfactant. Coalescence is controllably induced when a pair of drops passes through an electric field. As a demonstration, we measure reaction kinetics by adding a drop containing a substrate to a second drop containing an enzyme.

The microfluidic device is fabricated using standard soft lithography methods.⁵ A channel pattern of 25- μm -thick and 50- μm -wide negative photoresist is produced by UV photolithography on a silicon wafer. A mixture of polydimethylsiloxane (PDMS) elastomer and cross-linker with a ratio of 5:1 by weight is molded onto the channels and peeled off after being partially cured. Another mixture with a ratio of 20:1 by weight is spin cast at 3000 rpm to a 30 μm film on a glass substrate, on which are patterned indium tin oxide (ITO) electrodes.⁶ The film is also partially cured and bonded to the PDMS mold; the device is then fully cured, enhancing the bond between the two PDMS layers.⁷ A schematic cross section of the coalescence region of the microfluidic device is shown in the inset of Fig. 1.

We use this device to produce water drops in hexadecane (viscosity $\eta_{\text{oil}} = 3.4 \times 10^{-3}$ Pa s; density of 0.773 g/ml). We add 5 wt % surfactant (Span80) to prevent spontaneous drop

^{a)}Electronic mail: weitz@deas.harvard.edu

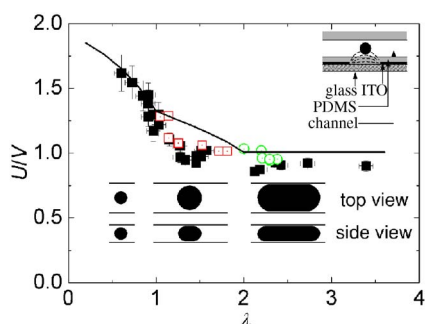


FIG. 1. (Color online) Drop velocities divided by the average velocity of the fluids injected as a function of the drop length divided by channel height. The filled symbols represent drop velocities measured before merging and the open symbols represent drop velocities after merging two streams of different-sized drops. The solid line is fluid velocity averaged across the cross-sectional area of the drop in the Poiseuille profile. The lower inset shows side and top views of drops depending on their size. The upper inset shows a cross-sectional schematic of the channel with the electrodes.

coalescence. The size of the water drops is controlled by adjusting the flow rates of the oil and water using syringe pumps (Harvard Apparatus).⁸ Water drops are produced with radii from 13 to 50 μm using water flow rates from 5 to 80 $\mu\text{l/h}$ and oil flow rates from 100 to 200 $\mu\text{l/h}$. Drop movement is recorded by a high-speed camera at a frame rate of 10 kHz to determine the relationship between drop size and velocity.

Water drops flow with different velocities depending on their size and shape. Due to their surface tension, the drops are spheres when their diameter is smaller than the channel height of 25 μm . As their diameter gets larger than 25 μm , their shape is constricted by the channel, and they attain a pancakelike shape. Above 50 μm , they are constricted by all four sides of the rectangular channel and they become plug-like in shape. Drops move more slowly as their size gets bigger, and plug-shaped drops have almost size-independent flow velocity. We summarize this dependence of the measured drop velocity U normalized by the average velocity of the fluid, V , on λ , the drop length normalized by the channel width, in Fig. 1.

Drop flow in rectangular channels is slightly different from that in cylindrical tubes,^{9–11} where drops have only spherical and pluglike shapes because of axial symmetry and where their velocity decreases with the square of their size,⁹ following the parabolic flow pattern in the cylindrical tubes. As a first approximation, this size-dependent drop velocity dispersion can be understood by considering the flux of liquid passing through a cross-sectional area since the drops are pushed by continuous phase liquid behind them. As a result, the drop velocity can be approximated as the average of the parabolic velocity profile across the drop cross section. The velocity profile in the absence of drops is $u_z(r) = A(d^2 - r^2)$; thus, the drop velocity is $U(R) = \int_0^R u(x, y) 2\pi r dr / \pi R^2 = A(d^2 - R^2/2)$, where d is radius of the pipe and A is a constant determined by the pressure gradient and viscosity. This result correctly accounts for the parabolic dependence of drop velocity on size. Thus, for example, the smallest drops have velocities similar to the maximum continuous phase velocity, whereas big drops, with the same diameter as the pipe, have velocities similar to that of the average velocity of the Poiseuille flow, which is half of the maximum. By analogy, we can understand drop flow in rectangular channels. From a

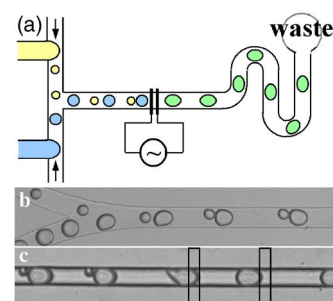


FIG. 2. (Color online) (a) Schematic view of the device. Water drops with two different sizes are independently formed using two T junctions and are merged into a single channel. After a small drop catches up with a big drop they are coalesced by an electric field. The coalesced drops travel along a long delay channel, allowing observation of chemical reactions inside the drops as a function of time. (b) An image showing streams of drops with two different sizes being merged and synchronized. The two different drops are generated at about the same rate by adjusting oil and water flow rates in each T junction. (c) Drops being coalesced by an electric field when they pass the electrodes. The locations of the transparent ITO electrodes have been indicated as rectangles.

Poiseuille profile, $u_z(x, y)$, in a rectangular channel in the absence of drops,¹² the velocity of a drop located in the center is given by $U(l) = \int^{A(l)} u_z(x, y) dx dy / A(l)$, where $A(l)$ is the cross-sectional area of a drop of length l and where the integration extends over $A(l)$. For spheres, A is proportional to l^2 , for pancake-shaped drops, it is linear in l , while for plug-shaped drops, it is independent of l . The result does not have an analytic solution so results of a numerical calculation are plotted as a solid line in Fig. 1. The results are in reasonable agreement with the data, but overestimate the experimentally measured velocities in the pancake and plug regimes. This may result from the fact that the approximation does not include the effects of the change in drop shape due to the shear forces or the modification of the velocity profile due to the presence of other drops in the channel. The discrepancy between theory and experiment may also be due to drops being located off center in the channel due to the density mismatch between the fluids, or due to the flow of the continuous fluid phase around the drops through the corners of the rectangular channel.

This size-dependent drop velocity dispersion can be used as a passive means of synchronization of drops. A microfluidic device using this concept is shown in Fig. 2(a). Two streams of drops, each of different sizes, are formed by independent T junction⁸ and are merged into a single channel. Due to the velocity dispersion, the smaller drops will always flow faster and catch up to the larger ones, thereby becoming synchronized. By ensuring that the production frequency of the smaller drops is slightly greater than that of the larger drops, there will always be at least one small drop paired with a large one; occasionally there will be two. The pairs of drops in contact do not coalesce because they are stabilized by surfactant. The synchronized drops can then be coalesced by applying an electric field.¹³

To illustrate the operation of this device, drops with two different diameters, about 50 and 25 μm , are produced and merged into the single channel. The rate of drop formation at both T junctions is fixed at 100 Hz. The smaller drop catches up to the larger one within 1 mm; this length depends on the initial spacing between drops and their velocity difference [Fig. 2(b)]. Under our experimental conditions, this takes less than 100 ms. The coalescence region is created with two

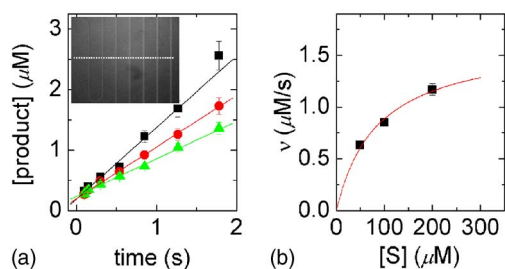


FIG. 3. (Color online) (a) Fluorescent intensity as a function of time at different substrate concentrations. The solid lines are linear fits to obtain reaction rates. The inset shows a fluorescence image of the delay channel with 4 s exposure time, which averages fluorescence from about 400 drops. The error bars are the standard deviations of ten replicates. (b) Michaelis-Menten plot of the reaction rates as a function of the substrate concentration. The error bars fall within the symbols.

parallel electrodes oriented perpendicular to the flow direction; these generate electric field parallel to the flow direction and aligned with the drop pair, as shown in Fig. 2(c). This alignment of the field induces the maximum force to deform the adjacent surfaces of the drops and is most effective for electrocoalescence.¹³ The electrodes are positioned sufficiently downstream from the drop merging point (1 cm) to ensure that each large drop flows in contact with one small drop as the pair enters the electric field region. An electric field generated by applying 100 V ac at 1 kHz across electrodes spaced 200 μm (500 kV/m) is sufficient to ensure coalescence of all drops.

To demonstrate the utility of this method for assays that require precise initiation timing, we determine the kinetic constants of the enzyme β -galactosidase from *E. coli* (EC 3.2.1.23). We make one stream of 25 μm drops which contain purified β -galactosidase (Sigma) at a concentration of 25 nM (3 nM in the coalesced drop) in 100 mM sodium phosphate pH 7.3 and 0.05% Tween-20. The second stream has 50 μm drops containing the fluorogenic substrate resorufin- β -D-galactopyranoside (RG) (Invitrogen) in the same buffer. After coalescence, the drops flow through a serpentine channel that allows us to image 2 s of reaction progress, and we record ten fluorescence-microscope images with a 4 s exposure [excitation/emission (ex/em) 530nm/590 nm], during each of which 400 drops pass each point of the channel. We use densitometry of the image to measure the reaction progress as reflected by the increasing fluorescence from the hydrolysis of RG by the enzyme [Fig. 3(a) inset]. To calibrate pixel intensities with concentrations

of resorufin we make drops containing 5 μM resorufin in the same buffer and image them in the same fashion. We perform the experiment with substrate concentrations of 60, 120, and 240 μM (50, 100, and 200 μM in the coalesced drop) [Fig. 3(a)]. Higher concentrations of substrate are not possible to assay due to the low solubility of RG in water. We plot the initial rates against the substrate concentrations in Fig. 3(b), and determine the turnover rate (k_{cat}) and Michaelis constant (K_M , apparent dissociation constant of the enzyme-substrate complex) to be 760 s^{-1} and 140 μM , respectively, by fitting to the Michaelis-Menten equation: $v = ([E]_0[S]k_{\text{cat}})/(K_M + [S])$ where v is the initial rate, $[E]_0$ is the enzyme concentration, and $[S]$ is the substrate concentration. These values are similar to previously reported values for k_{cat} and K_M of 730 s^{-1} and 350 μM , respectively.¹⁴

This method allows precise, programed control over the coalescence of drops at rates of thousands per second. It can be applied to high-throughput screening applications, such as combinatorial libraries of druglike molecules or gene encoding proteins. Our microfluidic drop coalescence devices can be used as an essential component in a platform for high-throughput screening bioassays.

This work was supported by a Human Frontiers grant and by the NSF (DMR-0243715) and through the Harvard MRSEC (DMR-0213805). The authors thank H. Stone for helpful discussion. INEST Group is sponsored by PMUSA.

¹H. Song, J. D. Tice, and R. F. Ismagilov, *Angew. Chem., Int. Ed.* **42**, 768 (2003).

²B. Zheng and R. F. Ismagilov, *Angew. Chem., Int. Ed.* **44**, 2520 (2005).

³D. R. Link, E. Grasland-Mongrain, A. Duri, F. Sarrazin, Z. Cheng, G. Cristobal, M. Marquez, and D. A. Weitz, *Angew. Chem., Int. Ed.* **45**, 2556 (2006).

⁴L.-H. Hung, K. M. Choi, W.-Y. Tseng, Y.-C. Tan, K. J. Shea, and A. P. Lee, *Lab Chip* **6**, 174 (2006).

⁵J. C. McDonald, D. C. Duffy, J. R. Anderson, D. T. Chiu, H. K. Wu, O. J. A. Schueller, and G. M. Whitesides, *Electrophoresis* **21**, 27 (2000).

⁶K. Ahn, C. Kerbage, T. P. Hunt, R. M. Westervelt, D. R. Link, and D. A. Weitz, *Appl. Phys. Lett.* **88**, 024104 (2006).

⁷M. A. Unger, H. P. Chou, T. Thorsen, A. Scherer, and S. R. Quake, *Science* **288**, 113 (2000).

⁸T. Thorsen, R. W. Roberts, F. H. Arnold, and S. R. Quake, *Phys. Rev. Lett.* **86**, 4163 (2001).

⁹B. P. Ho and L. G. Leal, *J. Fluid Mech.* **71**, 361 (1975).

¹⁰F. P. Bretherton, *J. Fluid Mech.* **10**, 166 (1961).

¹¹G. Hetsroni, S. Haber, and E. Wacholde, *J. Fluid Mech.* **41**, 689 (1970).

¹²R. E. Langlois, *Slow Viscous Flow* (Macmillan, New York, 1964).

¹³J. S. Eow and M. Ghadiri, *Colloids Surf., A* **219**, 253 (2003).

¹⁴J. Hofmann and M. Sernetz, *Anal. Chim. Acta* **163**, 67 (1984).